Magnetic flux shielding in superconducting strip arrays

P. Fabbricatore, S. Farinon, and S. Innocenti
Istituto Nazionale di Fisica Nucleare, Sezione di Genova, Via Dodecaneso 33, 16146 Genova, Italy

F. Gömöry
Institute of Electrical Engineering, Slovak Academy of Sciences, Dubravska cesta 9, 84239 Bratislava, Slovak Republic
(Received 2 June 1999; revised manuscript received 10 September 1999)

Meissner shielding in arrays composed of parallel diamagnetic strips has been studied when the field is applied normally to the wide face of strips. The numerical solution of the Laplace equation has been found using a commercially available finite-element code for electrical and magnetic analysis. First, the code application has been tested on simple structures such as a single ellipsoid or rectangular strip in a transverse field. Then, a regular two-dimensional array of parallel strips has been considered. The results of the computation can be approximated by simple empirical formulas for the magnetic susceptibility of such an array. As the last step, typical filament configurations of two real BiSrCaCuO-2223 multifilamentary tapes have been studied and the susceptibilities in the Meissner state calculated. We found that the regularity in filament distribution can dramatically influence the magnetic properties and consequently the magnetic ac losses in the tape.

I. INTRODUCTION

The technology of superconducting Ag/Bi2223 multifilamentary tapes has made much significant progress at the industrial level that they are more and more becoming commercially available for a wide class of applications. In this framework, the modeling of the electromagnetic properties of the tape in an applied field (dc or ac) is of basic importance. As a first approximation, one can represent the multifilamentary tape as an array of strips with a rectangular cross section. The aspect ratio of these strips is typically greater than 10; therefore, the models worked out for a infinite slab in a parallel field can be naturally applied only when the external field is parallel to the tape wide face. In this parallel configuration the ''end effects'' related to the lost of translational symmetry near the sample ends are commonly neglected. The situation with the external field applied perpendicularly to the tape is much more complicated. This can be illustrated by the results for a disk,[1] strip,[2] and infinite array.[5] However, the arrangement with a finite number of strips in the array, which at best corresponds to a multifilamentary tape, remains unsolved yet. The main difficulty in treating the perpendicular configuration is related to the fact that the end effects become prevalent in such a way that one can hardly distinguish them from the intrinsic properties of the superconductor. One possible way of separating the shape effects from the behavior of the superconducting material itself is to express the measured susceptibility—evaluated in the same way as for the parallel configuration and called the external susceptibility χ_{ext}—as a product of the internal susceptibility χ and a constant χ_0: $\chi_{\text{ext}} = \chi_0 \chi$. In the internal susceptibility χ, the response of superconductor to changes of, e.g., temperature or magnetic field is included. Therefore, this quantity can change from 0 in the normal state to -1 in the case when a sample with dimensions much larger than the London penetration depth is completely shielded. Thus in the Meissner state $\chi_{\text{ext}} = -\chi_0$ and this indicates that the constant χ_0 can be found both experimentally (at low temperature) and theoretically (by calculating the field distribution in body with ideal diamagnetic properties). The calculation of χ_0 strongly affects the ac loss evaluation. This is because the experimental calibration is valid only for samples with identical shapes. For this reason, distinguishing between external and internal susceptibility has important practical consequences: the measured susceptibility data can be scaled to the internal susceptibility span from 0 to -1, and then multiplied by χ_0 to determine χ_{ext}. From χ'', the imaginary part of the ac susceptibility, the loss volume density,[1] is obtained through

$$q_m = \pi \chi'' \chi_0 \frac{B_a^2}{\mu_0}, \tag{1}$$

where B_a is the ac field amplitude. Crucial at this point is knowledge of χ_0. A mistake in the determination of this quantity can induce large errors in the ac loss evaluation from the susceptibility data. The situation is further complicated in the case of multifilamentary tape, when in an ac magnetic field the currents flowing across the matrix can contribute to sample magnetization. In certain circumstances these currents prevail and one can consider the whole filamentary zone (see Fig. 1) with dimensions $2L \times d$ as a su-

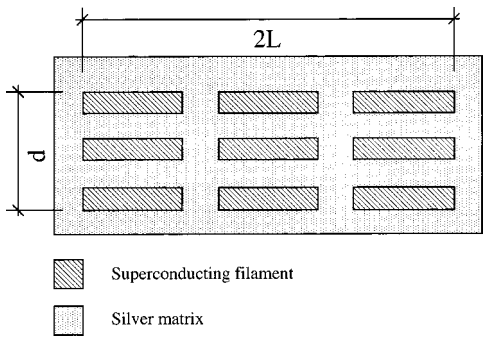

FIG. 1. Filamentary zone.

perconducting bulk. Then, the model of a superconducting strip in a perpendicular field[2] can be used and $\chi_0 = \pi L/2d$. On the other hand, very often the interfilament currents were found to be negligible in ac susceptibility experiments.[3] Then, the tape must be considered as an array of individual superconducting strips, where an interaction between screening currents in different strips takes place.

In the present paper we have studied the possibility of applying a standard numerical technique to this kind of problems. In particular the use of the commercially available finite-element (FE) code ANSYS (Ref. 4) has been investigated. As the first step the current and field distribution in a simple diamagnetic body (disk, strip) in a transverse field has been solved and compared with the classical magnetostatic solution. As the second step, an infinite stack of strips has been considered and compared with existing theories for transverse field penetration.[5] As the third step, regular arrays of strips have been analyzed. As the last step, the real filament configuration of the superconducting strips composing a multifilamentary BiSrCaCuO-2223 tape has been studied and the external susceptibility computed.

II. APPLICATION OF THE FE CODE ANSYS TO MEISSNER SHIELDING PROBLEMS

Generally speaking, the Meissner shielding in superconductors is given by surface currents flowing in a surface layer of a given London depth λ. From the magnetostatic point of view, this situation can be studied solving the Laplace equation[6] $\Delta\phi = 0$, for the magnetic scalar potential ϕ, defined as $\mathbf{H} = \nabla\phi$, with suitable boundary conditions. This can be easily done in some cases involving the simple geometry derived from that of an ellipsoid, as we will see in the next section. For more complex geometrical shapes, an analytical solution could not be found. We can take advantage of the fact that codes exist to solve the Laplace equation for any geometrical arrangement of magnetic materials. Though these codes were developed for high-magnetic-permeability material (such as iron), we can try to apply them in shielding problems assuming that the magnetic permeability in the material is $\mu_r = 0$, so that $B = 0$ inside the material for any applied field H_a. In making this simplification of the problem, we have to stress two points

(i) The local field generated by the shielding currents can be so high as to exceed H_{C1}, so that we have a local penetration of the magnetic flux. In the present paper, we assume that the external field is so low that it never exceeds H_{C1}.

(ii) For ferromagnetic materials, the magnetization is produced by microscopic currents, while for superconductors the shielding currents have a different nature. They are macroscopic and can generate a field H_i inside the materials, so the magnetization is found as the difference between internal field H_i and external field H_e, the latter being defined as $H_a[1/(1-D)]$ (where D is the demagnetizing factor). However, for our aim, this only means that in using finite-element codes made for ferromagnetic materials, we have to take care that the dimensions of the considered superconducting structures are much larger than the London penetration depth.

Provided that the two above points are taken into consideration, let us proceed to discuss the approach with the finite-element codes.

Generally speaking, we deal with a diamagnetic body of given dimensions and very low permeability ($\mu_r \sim 10^{-10}$) immersed in a uniform magnetic field $\mathbf{H}_a = H_a\mathbf{z}/z$. We are interested in information about the shielding current distribution, field distribution, and magnetic susceptibility. As we will see in the practical examples shown in the following sections, through a finite-element code we can obtain $\mathbf{H} = \mathbf{H}(\mathbf{r})$ in a given network (nodes). From knowledge of the field on the body surface, we can compute the surface shielding current $\mathbf{J}(\mathbf{r})$ using Ampère's law. The magnetic momentum is then obtainable as $\mathbf{m} = \frac{1}{2}\int \mathbf{r} \times \mathbf{J}(\mathbf{r}) dV$, from which the magnetic susceptibility is derived dividing it by the body volume and the applied field. In applying this process, we must pay attention to the problem symmetry. While for two-dimensional (2D) axis-symmetric cases (disks, rotational ellipsoids) the magnetic momentum is completely determined by the computed $\mathbf{J}(\mathbf{r})$ distribution, for a striplike geometry, analyzed with a 2D approach, we obtain only one-half of the true magnetic momentum and therefore multiply the obtained magnetic momentum by a factor of 2. This is because the currents flowing at the far-away ends of the strip are not considered in our 2D calculation.

A self-consistency check here is done computing the energy of the system, which is a simple task when using a finite-element code. Actually, we can consider the energy variation when a body of magnetic permeability μ_r is introduced in a medium of magnetic permeability μ_0 immersed in a uniform magnetic field H_a. This energy variation is given by[6]

$$\Delta W = -\frac{1}{2\mu_0}\int_{V_S} \mathbf{M}\cdot\mathbf{H}_a dV, \tag{2}$$

where V_S is the volume occupied by the sample. Since in the case of perfect shielding the magnetization of the body is constant, Eq. (2) can be rewritten as

$$\Delta W = -\frac{1}{2\mu_0} M H_a V_S, \tag{3}$$

from which χ_0 can be calculated as

$$\chi_0 = -\frac{M}{H_a} = \frac{\Delta W}{(1/2\mu_0)H_a^2 V_S} = \frac{\Delta W}{W_S}. \tag{4}$$

We found that the values of the magnetic susceptibility calculated using Eq. (4) and from the magnetic momentum agree perfectly; thus, in the following sections, we do not specify which of these two methods has been adopted.

III. DISK AND STRIP IN A TRANSVERSE FIELD

With the aim of finding how a transverse magnetic field is shielded by real multifilamentary tapes, we start analyzing a simple structure like disks and strips.

All the current theories about transverse field penetration in tapes are based on the Landau approach.[7] The shielding current distribution is calculated for an ellipsoid in the limit of extremely thin thickness ($R \gg d$, where R and $d/2$ are, respectively, the major and minor semiaxes). For a diamag-

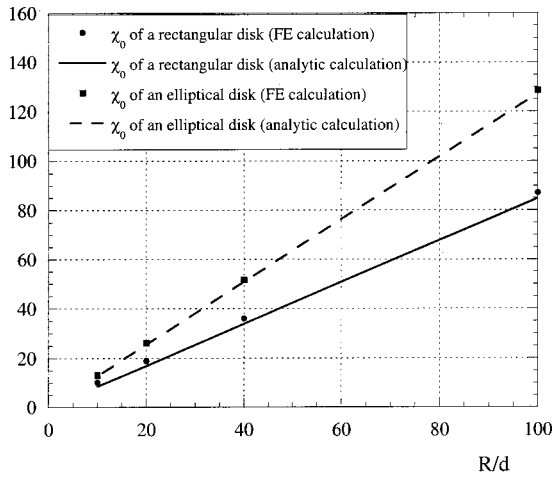

FIG. 2. Comparison of χ_0 analytically and numerically calculated for a disk with an elliptical (major semiaxis R, minor semiaxis $d/2$) and rectangular (radius R, thickness d) section as a function of R/d.

netic disk placed in a uniform transverse magnetic field $\mathbf{H}_a = H_a \mathbf{z}/z$, the current distribution averaged over the thickness of the disk is

$$J(\rho<R) = -\frac{4}{\pi d} H_a \frac{\rho}{\sqrt{R^2-\rho^2}}, \tag{5}$$

and the z component of the field in the $z=0$ plane is[1]

$$H(\rho>R) = H_a \left\{ 1 + \frac{2}{\pi} \left[\frac{1}{\sqrt{(\rho/R)^2-1}} - \sin^{-1}\left(\frac{R}{\rho}\right) \right] \right\}. \tag{6}$$

Using Eq. (5), one can find an expression of the magnetization and susceptibility:

$$M = \frac{m_z}{\frac{4}{3}\pi R^2 d/2} = -\frac{4}{\pi} H_a \frac{R}{d}, \quad \chi_0 = -\frac{M}{H_a} = \frac{4}{\pi}\frac{R}{d}. \tag{7}$$

The current and field distribution given by Eqs. (5) and (6) is valid also for a diamagnetic disk with a rectangular cross section (radius R and constant thickness d). Because of different sample volumes, we obtain now

$$M = \frac{m_z}{\pi R^2 d} = -\frac{8}{3\pi} H_a \frac{R}{d}, \quad \chi_0 = -\frac{M}{H_a} = \frac{8}{3\pi}\frac{R}{d}. \tag{8}$$

We have verified these expressions through the ANSYS code computing χ_0 and comparing with the values given in Eqs. (7) and (8) for different ratios R/d, as shown in Fig. 2. Though the agreement is quite good, for the disk we have found some differences coming from the current paths. In fact, there are two contributions to the magnetic momentum: one comes from the currents flowing on the upper and lower surfaces of the disk (J_{UL}) and a second one coming from the side currents (J_S). Starting from the field computed by ANSYS, we have calculated the two current distributions which the analytical solution, based on thin ellipsoid, cannot take into account separately. Actually, even for the thinnest disks with a rectangular cross section, both J_{UL} and J_S do contribute to the magnetization. Figure 3 shows J_{UL}, J_S, and J_E, the latter being the current density coming from Eq.

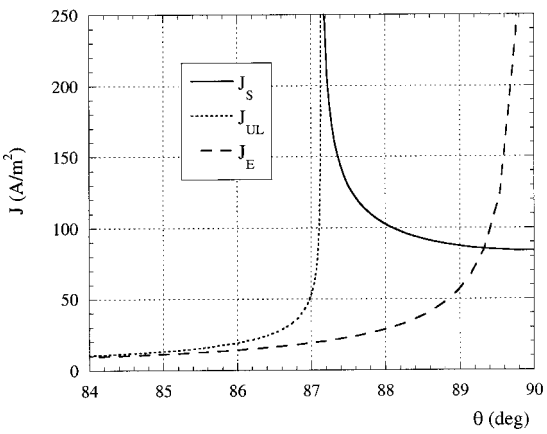

FIG. 3. Enlargement in the corner region of the current densities J_E, J_{UL}, and J_S as a function of the polar angle θ. J_E is the current density of the rotational ellipsoid; J_{UL} and J_S are, respectively, the upper (or lower) and side current densities of the rectangular cross section disk.

(5), as a function of the polar angle θ. It is striking that in spite of such a difference in the distribution pattern the used approximation gave reasonable results for χ_0.

As the next step, let us consider a diamagnetic strip of infinite length in the y direction and an ellipsoidal cross section (semiaxes L and $d/2$) in the xz plane, $x^2/L^2 + z^2/(d/2)^2 = 1$. A constant field H_a is applied along z. As the first step, we have found the general analytical expressions for the current density and the magnetic field of the strip. Following the approach proposed by Landau and Lifshitz[7] for a rotational ellipsoid, the current distribution averaged over the thickness of the strip can be found as

$$J(x<L) = -\frac{2\alpha}{d} H_a \frac{x}{\sqrt{k^2-x^2}}, \tag{9}$$

where

$$\alpha = \sqrt{\frac{1+d/2L}{1-d/2L}} \quad \text{and} \quad k^2 = \frac{L^2}{1-(d/2L)^2}.$$

We have also found an approximated expression for $H(x>k)$:

$$H(x>k) = 1 + \frac{2\alpha}{\pi}\left[-\arctan\left(\frac{2L^2}{kd}\right) + \frac{x}{\sqrt{x^2-k^2}} \arctan\left(\frac{2L^2}{kd}\frac{\sqrt{x^2-k^2}}{x}\right)\right]. \tag{10}$$

Repeating the procedure outlined in calculating the susceptibility of disk, for a strip with a current distribution given by Eq. (9) one obtains the external magnetic susceptibility

$$\chi_0 = \frac{2\alpha L}{d}. \tag{11}$$

In the limit of a thin strip ($d/2L \to 0$, i.e., $\alpha \to 1$ and $k \to L$) this expression coincides with the solution used by Brandt:[2]

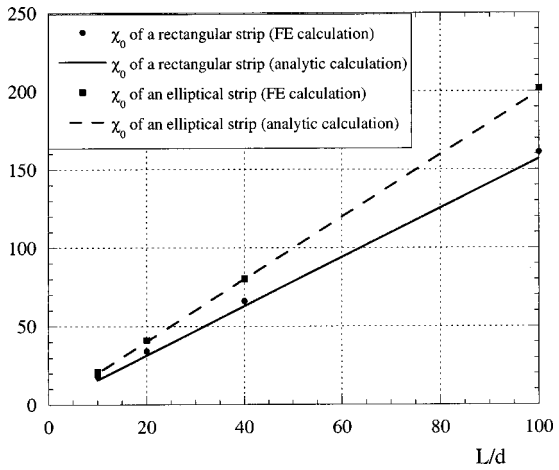

FIG. 4. Comparison of χ_0 analytically and numerically calculated for rectangular and elliptical cross section strips as a function of L/d.

$$J(x<L)=-\frac{2}{d}H_a\frac{x}{\sqrt{L^2-x^2}}, \tag{12}$$

with the corresponding field distribution

$$H(x>L)=H_a\frac{x}{\sqrt{x^2-L^2}} \tag{13}$$

and magnetic susceptibility:

$$\chi_0=\frac{2L}{d}. \tag{14}$$

Similarly as for the disks, we can extend the results obtained for a thin elliptical strip to a rectangular one (width $2L$ and constant thickness d). In this case

$$\chi_0=\frac{\pi}{2}\frac{L}{d}. \tag{15}$$

A comparison of numerically and analytically calculated χ_0 for elliptical and rectangular strips is given in Fig. 4. As for disks, good agreement is found for the elliptical strip, while the slight difference in the rectangular strip case is again due to the fact that the magnetization is given by the two contributions of surface and side currents.

IV. z STACK OF STRIPS

As a conclusion of the previous sections, we found that χ_0 determined in a numerical way by ANSYS for a strip or a disk coincides with the corresponding analytical expression (8) or (15). This result allows us to apply the same approach to a set of striplike filaments. Let us consider a z stack of strips as shown in Fig. 5. Mawatari[5] has given an elegant formulation of this problem in case of a z stack made by an infinite number of strips. In the following, we compare our numerical approach with his analytical results:

$$J(x<L)=-\frac{2}{d}H_a\frac{\sinh(\pi x/D)}{\sqrt{\sinh^2(\pi L/D)-\sinh^2(\pi x/D)}}, \tag{16}$$

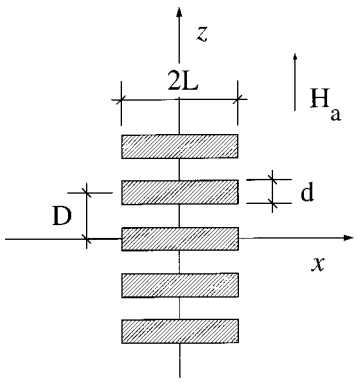

FIG. 5. Arrangement of strip lines in a z stack.

$$H(x>L)=H_a\frac{\sinh(\pi x/D)}{\sqrt{\sinh^2(\pi x/D)-\sinh^2(\pi L/D)}}, \tag{17}$$

from which χ_0 is calculated as

$$\chi_0=\frac{D^2}{\pi L d}\ln\left[\cosh\left(\frac{\pi L}{D}\right)\right]. \tag{18}$$

These formulas are not valid for a finite number of strips in the stack. We can take advantage of our numerical approach, which allows calculating the magnetization for a stack consisting of an arbitrary number of strips. Differently from an infinite stack, the magnetization now is not uniform, but changes with respect to the position of strip in the stack. Representative values can be calculated either by averaging on all the strips ($M_{\rm ave}$) or for the central strip of the stack ($M_{\rm cen}$). The latter should approach the result for an infinite stack by increasing the number of strips. This means that also for χ_0 we can obtain two different results: $\chi_{0\rm ave}=-M_{\rm ave}/H_a$ and $\chi_{0\rm cen}=-M_{\rm cen}/H_a$. For two different geometries, the dependence of numerically calculated χ_0 on the number of strips in the stack is given in Figs. 6(a) and 6(b) together with the analytical formula for an infinite stack. As expected, $\chi_{0\rm cen}$ approaches the result for an infinite stack when increasing the number of strips, while $\chi_{0\rm ave}$ represents the real value of the magnetic susceptibility of the finite z stack as a function of the strip number.

In order to compare different values of $\chi_{0\rm ave}$ as a function of the geometrical parameters (L, d, and D), it is useful to normalize it in the range 0–1:

$$X_{0\rm ave}=\frac{\chi_{0\rm ave}-\chi_0(\infty)}{\chi_0(1)-\chi_0(\infty)}, \tag{19}$$

where $\chi_0(1)$ and $\chi_0(\infty)$ are, respectively, the magnetic susceptibility of one strip [Eq. (15)] and of an infinite number of strips [Eq. (18)]. From a very general point of view, piling n strips with no gap in between ($D=d$), the susceptibility is simply given by

$$\chi_0=\frac{\pi}{2}\frac{L}{d}\frac{1}{n}. \tag{20}$$

For this reason, it is not surprising to find that the normalized magnetic susceptibility $X_{0\rm ave}$ as a function of the number of strips n, is well fitted by a decreasing exponential:

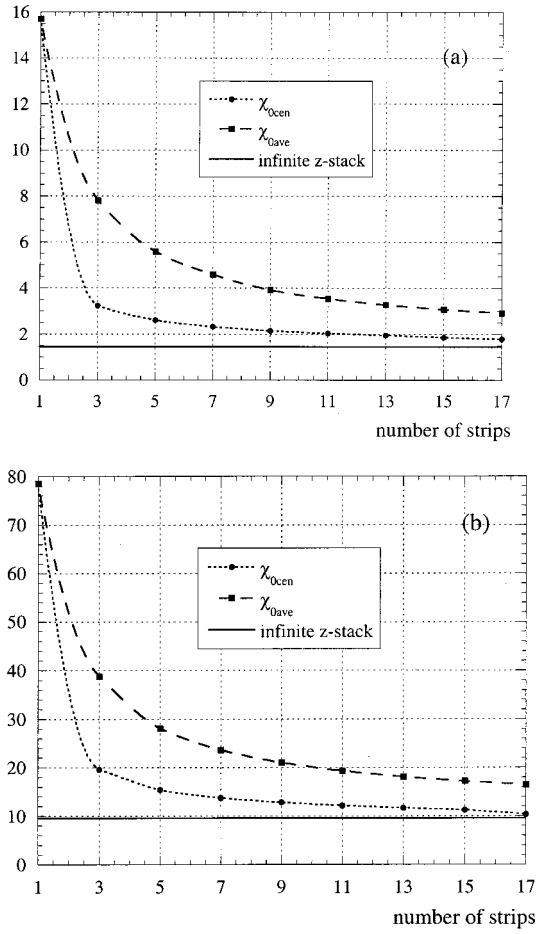

FIG. 6. Dependence of a numerically calculated χ_0 on the number of strips in the z stack together with an analytical formula for an infinite stack for two different geometries: (a) $L=100\ \mu$m, $d=10\ \mu$m, $D=15\ \mu$m; (b) $L=100\ \mu$m, $d=2\ \mu$m, $D=20\ \mu$m.

$$X_{0\text{ave}}=\frac{1}{n^{\alpha}}, \tag{21}$$

where α should be close to unity. We have found that for real conductors, where $L/d>5$ and $L/(D-d)>20$, α assumes a constant value of about 0.8. Finally, it is possible to estimate the magnetic susceptibility of a z stack when the number of strips is greater than 1, but much less than infinity:

$$\chi_{0\text{ave}}(n)\approx\chi_0(\infty)+\frac{\chi_0(1)-\chi_0(\infty)}{n^{0.8}}. \tag{22}$$

V. x ARRAY OF STRIPS

Let us now consider a plane array of diamagnetic strips as shown in Fig. 7. Following Mawatari's approach,[5] the current density and magnetic field of an infinite x array are, respectively,

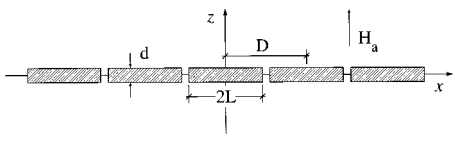

FIG. 7. Arrangement of strip lines in an x array.

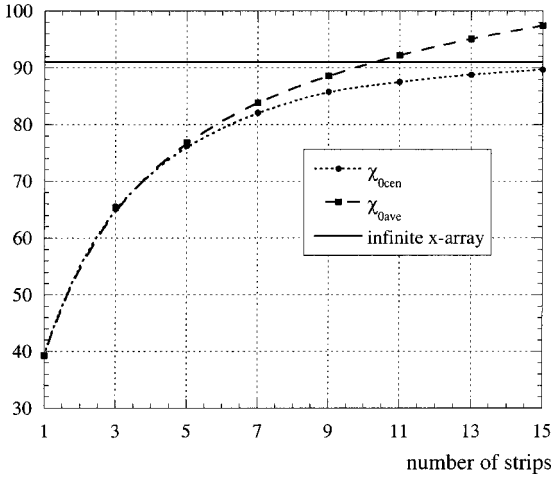

FIG. 8. Dependence of numerically calculated χ_0 on the number of strips in the x array together with an analytical formula for an infinite stack, for a strip of dimensions $L=50\ \mu$m, $d=2\ \mu$m, $D=105\ \mu$m.

$$J(x<L)=-\frac{2}{d}H_a\frac{\sin(\pi x/D)}{\sqrt{\sin^2(\pi L/D)-\sin^2(\pi x/D)}}, \tag{23}$$

$$H(x>L)=H_a\frac{\sin(\pi x/D)}{\sqrt{\sin^2(\pi x/D)-\sin^2(\pi L/D)}}, \tag{24}$$

from which χ_0 is calculated as

$$\chi_0=-\frac{D^2}{\pi L d}\ln\left[\cos\left(\frac{\pi L}{D}\right)\right]. \tag{25}$$

For an x array consisting of a finite number of strips, an analytical solution does not exist and a numerical approach has to be used. One expects that the current and field distribution will no longer be periodic. Then, the magnetization of the central strip will differ from the averaged magnetization of all the array, resulting in a corresponding difference in averaged susceptibility $\chi_{0\text{ave}}$ and that calculated for the central strip, $\chi_{0\text{cen}}$.

As is clear from Fig. 8, $\chi_{0\text{ave}}$ of an x array does not approach Mawatari's expression when increasing the number of strips. We think that this discrepancy is due to the currents flowing at the strip sides (J_S). In the x array each strip must shield the applied field plus the field generated by the currents in neighbor strips. The most efficient way to shield the extra field generated by the neighbor strips is by the currents at strip sides. This causes the current distribution $J(\theta)$ to be significantly different from the one derived for an ellipsoid (with $d\to 0$) and put in the base of Mawatari's approach. This problem was not found in the z stack because in that case the currents in neighbor strips decrease the field to be shielded and consequently the contribution to the magnetization of the currents flowing at the strip sides (J_S) is decreased too.

As a consequence, we do not know *a priori* the limit of the averaged magnetic susceptibility for the number of strips which tends to infinity. In order to compare different values

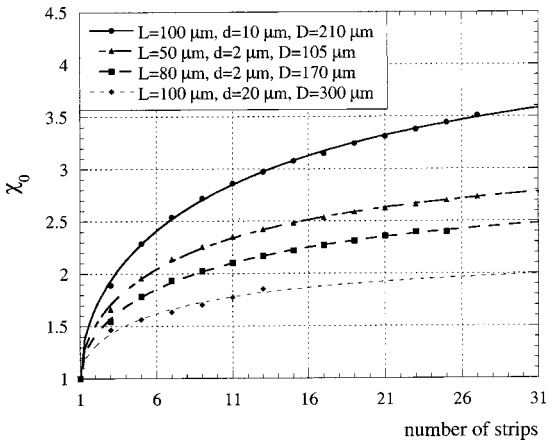

FIG. 9. Behavior of the normalized magnetic susceptibility of an *x* array as a function of the number of strips, for different strip geometries.

of $\chi_{0\text{ave}}$ as a function of the geometrical parameters (L, d, and D), we can anyway normalize it to the magnetic susceptibility of one strip $\chi_0(1)$:

$$X_{0\text{ave}}=\frac{\chi_{0\text{ave}}}{\chi_0(1)}. \tag{26}$$

The function $X_{0\text{ave}}$ should have the following behavior:

$$X_{0\text{ave}}=1+\frac{2}{\pi}(\beta-1)f(n), \tag{27}$$

where β represents the asymptotic value of the averaged magnetic susceptibility and could be calculated starting from Mawatari's limit [Eq. (25)] as

$$\beta\approx\frac{\chi_0(\infty)}{\chi_0(1)}, \tag{28}$$

and $f(n)$ is a function ranging from 0 to $\pi/2$ as n ranges from 1 to ∞.

In Fig. 9, $X_{0\text{ave}}$ as a function of the number of strips, n, is shown for different values of L, d, and D. As expected, we found that it is very well fitted by an expression similar to Eq. (27), at least for a reasonable number of strips:

$$X_{0\text{ave}}=1+\frac{2}{\pi}(\beta-1)\operatorname{arcsec}\left(\frac{n+n^*-1}{n^*}\right). \tag{29}$$

Nevertheless, the parameter β is different from Eq. (28). We have to take into account that Mawatari's approach is valid in the limit $d\to 0$ and $(D-2L)\to 0$. The first limit $d\to 0$ is obvious and comes directly from the thin ellipsoid approximation. The second one $(D-2L)\to 0$ comes from the consideration that the magnetic susceptibility of an infinite *x* array should be much higher than that of a single strip:

$$-\frac{D^2}{\pi L d}\ln\cos\frac{\pi L}{D}\gg\frac{\pi}{2}\frac{L}{D},\quad\text{with}\quad 0<\frac{\pi L}{D}\leqslant\frac{\pi}{2}. \tag{30}$$

That is true only if $\pi L/D\approx\pi/2$, i.e., $D\approx 2L$.

This leads us to modify Eq. (28) to the empirical expression

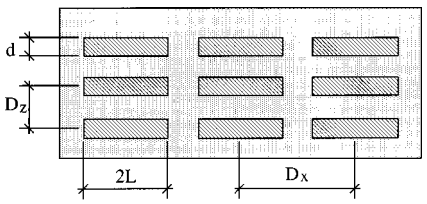

FIG. 10. Arrangement of a regular matrix of strips.

$$\beta=\frac{\chi_0(\infty)}{\chi_0(1)}\frac{D}{2L}\frac{d+(D-2L)}{(D-2L)}. \tag{31}$$

The function $f(n)$ is well represented by an arc secant function; in Eq. (29), the parameter n^* gives information on how fast the function converges to the asymptote. Surprisingly, we have found that n^* is related to β, i.e., $n^*\sim 5\beta$.

The fair agreement allows one to estimate the averaged magnetic susceptibility of an *x* array composed of a finite number of strips.

VI. *xz* ARRAY

It is now interesting to apply the previous empirical rules to a regular matrix of strips as shown in Fig. 10. Starting from the magnetic susceptibility of one strip and by applying subsequently the reducing factor due to the stacking in the *z* direction and the increasing factor due to the repeating in the *x* direction, we can suppose that the resulting magnetic susceptibility of the matrix is

$$\chi_0=\chi_0(1)\frac{f_x}{f_z}, \tag{32}$$

where

$$f_x=1+\frac{2}{\pi}(\beta-1)\operatorname{arcsec}\left(\frac{n_x+n^*-1}{n^*}\right),$$
$$f_z=\frac{\chi_0(1)}{\chi_0(\infty)+[\chi_0(1)-\chi_0(\infty)]/n_z^{0.8}}; \tag{33}$$

with n_x the number of strips in the *x* direction and n_z the number of strips in the *z* direction, $n^*=5\beta$, $\chi_0(1)$, $\chi_0(\infty)$, and β as described, respectively, by Eqs. (15), (18), and (31). Some results are summarized in Table I. We found that, if $D_z-d\lesssim d$ and $D_x-2L\lesssim 2L$, the differences between χ_0 calculated by ANSYS or using Eq. (32) are well under 10%. For comparison, Table I includes also the magnetic susceptibility calculated applying Eq. (15) to the overall dimensions $\tilde{L}$ and $\tilde{d}$ of the strip array:

$$\chi_{0,\text{ov}}=\frac{\pi}{2}\frac{\tilde{L}}{\tilde{d}}=\frac{\pi}{2}\frac{(n_x-1)D_x+2L}{(n_z-1)D_z+d}. \tag{34}$$

It is clear that this last method applied to regular arrays of strips induces very large errors in the evaluation of χ_0.

VII. REAL MULTIFILAMENTARY TAPES

As the next step, let us consider two real multifilamentary tapes with cross section shown in Fig. 11(a) (36-filament

TABLE I. Comparison of χ_0 calculated in different way for a regular array of strips.

Geometry	f_x	f_z	χ_0 calculated from Eq. (32)	χ_0 calculated by ANSYS	χ_0 calculated from Eq. (34)
$L=100\ \mu$m $d=20\ \mu$m $D_x=300\ \mu$m $D_z=25\ \mu$m $n_x=5$ $n_z=5$	1.599	2.599	4.832	4.651	18.326
$L=100\ \mu$m $d=10\ \mu$m $D_x=210\ \mu$m $D_z=15\ \mu$m $n_x=5$ $n_z=5$	2.324	2.917	12.515	13.182	23.338
$L=50\ \mu$m $d=2\ \mu$m $D_x=105\ \mu$m $D_z=4\ \mu$m $n_x=5$ $n_z=5$	1.961	3.203	24.043	25.767	45.379
$L=100\ \mu$m $d=20\ \mu$m $D_x=300\ \mu$m $D_z=25\ \mu$m $n_x=5$ $n_z=3$	1.599	1.987	6.320	6.098	31.416

tape[8]) and (b) (19-filament tape[9]). Modeling the filaments as strips with a rectangular cross section, the current and field distributions have been calculated using ANSYS. In Figs. 12(a) and 12(b) the resulting flux lines are shown. The calculated (ANSYS) values for the susceptibility are $\chi_0=7.5$ for the 36-filament tape and $\chi_0=34.6$ for the 19-filament tape. The empirical rule in Eq. (32) can only be applied to the 36-filament tape, having a regular rectangular x-z array of filaments, resulting in $\chi_0=4.0$. Two main considerations come from these results.

(i) A regular x-z array of filaments allows the field to penetrate into the tape structure, causing relatively low values of the magnetic susceptibility. This helps in limiting the effect of the demagnetizing field and consequently the ac losses. The 36-filament tape is a good example in this sense: in each 6-filament z stack, χ_0 is decreased, compensating the increase of χ_0 due to the x-array distribution. A hexagonal filament structure or a disordered structure (where no z stack is present as in 19-filament tape) constitutes a barrier to field penetration, causing a dramatic increase of the magnetic susceptibility.

(ii) Though the 36-filament tape has an x-z array struc-

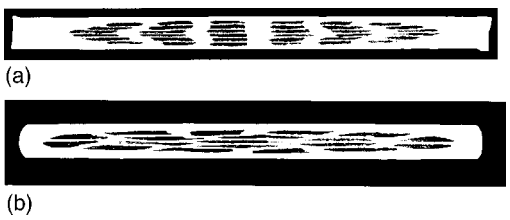

FIG. 11. Optical micrographs of two axially rolled 36-filament (0.22×2.0 mm^2) (a) and flat rolled 19-filament (0.14×2.5 mm^2), (b) tape.

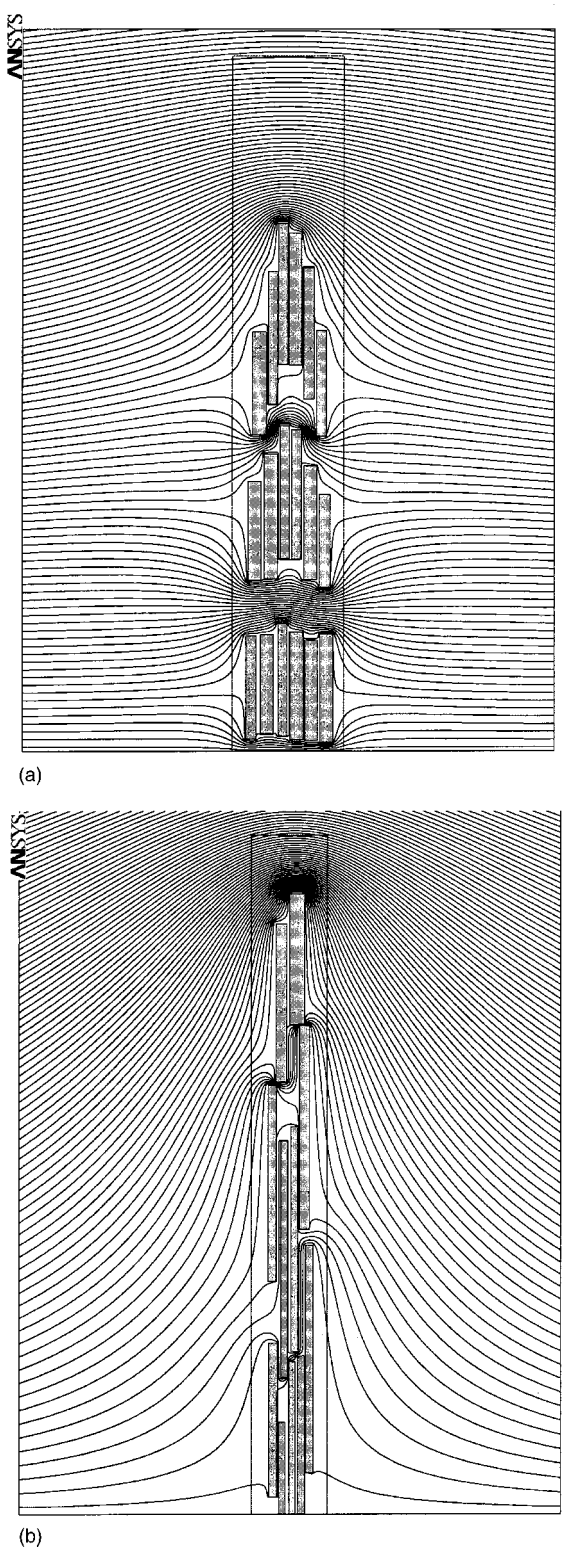

FIG. 12. Flux lines of the two real conductors, 36-filament tape (a) and 19-filament tape (b).

ture, we cannot apply Eq. (32) to predict with good accuracy the value of χ_0, due to the irregularities of the array. In this case we have to use the finite-element approach.

VIII. ac LOSSES

From a practical point of view, the regime of diamagnetic shielding has not attracted great attention because it is relevant at very small magnetic fields only. In applications counting on a high-current-carrying capacity of type-II superconductors with pinning, the critical state model[10] explains well the fundamental electromagnetic properties including ac loss. Systematic efforts lead to the derivation of ac loss formulas for the shapes that are close to the tape sample: disk and strip.[1,2] The ac loss density can be determined according to Eq. (1) from the ac susceptibility:

$$\chi''_{\text{tape}}=\frac{4}{\pi}\frac{B_p}{B_a}g\left(\frac{B_p}{B_a}\right), \tag{35}$$

$$\chi''_{\text{disk}}=\frac{2}{\pi}\int_0^{\pi}\left[-S\left(\frac{B_a}{B_p}\right)+(1-\cos\vartheta)S\left(\frac{B_a}{2B_p}(1-\cos\vartheta)\right)\right]\sin\vartheta\, d\vartheta, \tag{36}$$

where B_a is the peak applied field, B_p is the field at which we have the full penetration of the sample, $g(x)=(2/x)\ln\cosh x-\tanh x$, and

$$S(x)=\frac{1}{2x}\left[\cos^{-1}\left(\frac{1}{\cosh x}\right)+\frac{\sinh x}{\cosh^2 x}\right].$$

B_p is defined as a function of the bulk critical current density J_c:

$$B_{p,\text{disk}}=\frac{\mu_0 J_c d}{2},\quad B_{p,\text{strip}}=\frac{\mu_0 J_c d}{\pi}. \tag{37}$$

Often, the experimental data can be well fitted to these formulas also in the case of real tape with a certain distribution of filaments.[11] Then, instead of trying to calculate the critical state in a general multifilamentary tape, one can think to model it by an ''effective'' filament or disk. Then, for ac loss, we use one of these models with an appropriate proportionality constant for ac loss evaluation, χ_0. According to the tape complexity, the calculation of χ_0 represents a different level of complications. Real dimensions of the superconducting core are to be put in the formulas for χ_0 in the case of monocore tape. For a multifilamentary tape, the extent of the magnetic coupling between individual filaments has to be established. In the case the filaments are uncoupled, the dimensions of one filament seem to be representative. On the other hand, in the case of a strong magnetic interaction between filaments, the ''effective'' strip or disk should coincide with the dimensions and shape of the whole filamentary zone. There is no model available to calculate the magnetic coupling between filaments in a critical state. Then, we see as a valuable approximation the situation of diamagnetic shielding. The external susceptibility χ_0 is an integral characteristic that reflects both dimensions and interfilament coupling. In this paper, we demonstrated the importance of tools to compute the external susceptibility that scales the ac losses and, as we have seen, can get very high values (35 for the 19-filament tape).

Concluding, though the analysis of the shielding current cannot be used to calculate the losses coming from bulk current, it gives the much more important scaling factor for the losses.

IX. CONCLUSIONS

We have demonstrated that commercially available finite-element codes for magnetostatic problems can be applied for predicting the shielding in superconductors. This approach has been checked in the shapes derived from a rotational ellipsoid, for which analytical solutions are available. The study of field shielding in a single strip of rectangular cross section and by array of such strips in transverse field has shown the following.

(i) The shielding current distribution is different than in an ellipsoid. There is an important contribution to the magnetization of current flowing at the sides of the strip. However, the magnetic momentum calculated using the surface and side currents in the strip (or the disk) is equal to the momentum obtained considering the strip (disk) as an extremely thin ellipsoid.

(ii) The approximation of thin ellipsoid fails when considering an x array of strips, because of the large role of the shielding currents flowing at the strips sides.

(iii) Empirical formulas describing the magnetic susceptibility of finite z stacks and x arrays of strips have been found. These formulas have been composed for predicting χ_0 of an x-z array, giving in a simple way results that are within 10% of the values obtained by finite-element analysis.

(iv) Analysis of the shielding current and field distribution in real multifilamentary tapes showed that χ_0 grows considerably when the filament structure does not form a regular array.

(v) The external susceptibility χ_0 scales the ac losses with a large factor (up to 35 in one of our tapes). It can be computed only through finite-element analysis when we have a complex system like multifilamentary tapes. This factor is as important as the inner susceptibility χ'', for which several good theoretical approaches, based on the critical state model, exist.

[1] J. R. Clem and A. Sanchez, Phys. Rev. B **50**, 9355 (1994).
[2] E. H. Brandt, Phys. Rev. B **49**, 9024 (1994).
[3] F. Gömöry, L. Gherardi, R. Mele, D. Morin, and G. Crotti, Physica C **279**, 39 (1997).
[4] Computer code ANSYS, Revision 5.5, Swanson Analysis Systems, Inc., 1998.
[5] Y. Mawatari, Phys. Rev. B **54**, 13 215 (1996).
[6] J. D. Jackson, *Classical Electrodynamics* (Wiley, New York 1962).
[7] L. D. Landau and E. M. Lifshitz, *Electrodynamics of Continuous*

Media, Theoretical Physics, Vol. 8 (Nauka, Moscow, 1982).
[8] P. Kováč, I. Hušek, and L. Kopera, Supercond. Sci. Technol. **10**, 982 (1997).
[9] P. Kováč, I. Hušek, A. Rosova, and W. Pachla, Physica C **312**, 179 (1999).
[10] C. P. Bean, Phys. Rev. Lett. **8**, 250 (1962).
[11] F. Gömöry, L. Gherardi, G. Crotti, D. Bettinelli, L. Martini, L. Bigoni, and S. Zannella, Physica C **310**, 168 (1998).